Kusumi, A., Sakaki, T., Yoshizawa, T., & Ohnishi, S. (1980b) *J. Biochem. (Tokyo) 88*, 1103-1111.
Kusumi, A., Subczynski, W. K., & Hyde, J. S. (1982) *Fed. Proc., Fed. Am. Soc. Exp. Biol. 41*, 1394, Abstr. 6571.
Mason, W. T., & Abrahamson, E. W. (1974) *J. Membr. Biol. 15*, 383-392.
O'Brien, D. F., Costa, L. F., & Otto, R. A. (1977) *Biochemistry 16*, 1295-1303.
Oosawa, F. (1973) *J. Theor. Biol. 39*, 373-386.
Oosawa, F. (1975) *J. Theor. Biol. 52*, 175-186.
Osborne, H. B. (1976) *FEBS Lett. 67*, 23-27.
Pober, J., & Stryer, L. (1975) *J. Mol. Biol. 95*, 477-481.
Pontus, M., & Delmelle, M. (1975) *Exp. Eye Res. 20*, 599-603.
Popp, C. A., & Hyde, J. S. (1981) *J. Magn. Reson. 43*, 249-258.
Rousselet, A., Cartand, J., & Devaux, P. F. (1981) *Biochim. Biophys. Acta 648*, 169-185.
Sanson, A., Ptak, M., Rigaud, J. L., & Gary-Bobo, C. M. (1976) *Chem. Phys. Lipids 17*, 435-444.
Shichi, H., & Shelton, E. (1974) *J. Supramol. Struct. 2*, 7-16.
Tsuda, M. (1979a) *Biochim. Biophys. Acta 578*, 372-380.
Tsuda, M. (1979b) *Biochim. Biophys. Acta 545*, 537-545.
Tsuda, M. (1982a) *Methods Enzymol. 81*, 392-399.
Tsuda, M. (1982b) *Biophysics (Kyoto)* (in press).
Tsuda, M., & Akino, T. (1981) *Biochim. Biophys. Acta 643*, 63-75.
Tsuda, M., Tokunaga, F., Ebrey, T. G., Yue, K. T., Marque, J., & Eisenstein L. (1980) *Nature (London) 287*, 461-462.
Yoshizawa, T. (1982) in *Handbook of Sensory Physiology VII/I Photochemistry of Vision* (Dartnall, J. H. A., Ed.) pp 146-179, Springer-Verlag, Berlin.

Interaction of Dipalmitoylphosphatidylcholine and Dimyristoylphosphatidylcholine-d_{54} Mixtures with Glycophorin. A Fourier Transform Infrared Investigation†

Richard A. Dluhy, Richard Mendelsohn,* Hector L. Casal, and Henry H. Mantsch

ABSTRACT: Glycophorin from the human erythrocyte membrane has been isolated in pure form and reconstituted into large unilamellar vesicles comprised of binary mixtures of 1,2-dipalmitoyl-3-*sn*-phosphatidylcholine (DPPC) and chain perdeuterated 1,2-dimyristoyl-3-*sn*-phosphatidylcholine (DMPC-d_{54}). The effect of temperature and protein on lipid structure and mixing was monitored by using Fourier transform infrared spectroscopy; deuteration of one of the components of the mixture permits observation of the protein interaction with each lipid species. The melting curves were analyzed by assuming that each lipid chain can exist in one of two physical states (i.e., gel or liquid crystalline), characterized by a temperature-dependent Lorentzian distribution for the line shape of the C-H or C-D stretching vibrations. The fraction of each lipid component melted at temperatures within the two-phase region of the phase diagram was calculated and approximate phase diagrams were constructed. Addition of protein lowers the liquidus line of the phase diagram while leaving the solidus line essentially unchanged. No lipid phase separation is observed. The effect of protein is more pronounced on the DPPC component than on the DMPC-d_{54}. The former is significantly more disordered and/or fluidized at all lipid mole fractions in the ternary system than in the binary phospholipid mixture.

Structural studies of lipid-protein interaction in reconstituted systems have provided basic information about the organization of biological membranes. Although many experiments have focused on the interaction of membrane proteins with a single lipid component [for a current overview, see Parsegian (1982)], less information is available for ternary systems consisting of a binary phospholipid mixture along with protein. Such experiments provide an opportunity to determine whether membrane proteins partition into regions of particular chemical structure or physical order in a complex lipid environment. The related question of lipid control of membrane protein function may also be investigated.

Several structural studies of ternary systems have appeared. Differential scanning calorimetry (DSC)[1] has been used to detect phase separation induced by lipophilin in mixtures of 1,2-dipalmitoyl-3-*sn*-phosphatidylcholine (DPPC) and phosphatidylserine (Boggs et al., 1977a,b), while Chapman et al. (1977) have investigated the partitioning of gramicidin A into 1,2-dilauroyl-3-*sn*-phosphatidylcholine-DPPC mixtures. At low concentrations, the polypeptide preferentially associated with the lower melting region of the bilayer whereas at higher levels a mixing of the two lipids was induced. Kleeman et al. (1974) used freeze-fracture electron microscopy to investigate the partitioning of glycophorin into two binary phosphatidylcholine mixtures. More recent spectroscopic studies include those of Verma et al. (1980) and Jonas & Mason (1981).

Fourier transform infrared (FT-IR) spectroscopy offers several advantages for the study of ternary systems. Vibrational spectra are sensitive to alterations in the conformation

† From the Department of Chemistry, Olson Laboratories, Newark College of Arts and Sciences, Rutgers University, Newark, New Jersey 07102 (R.A.D. and R.M.), and the Division of Chemistry, National Research Council of Canada, Ottawa, Ontario, Canada K1A 0R6 (H.L.C. and H.H.M.). *Received June 29, 1982; revised manuscript received December 1, 1982.* This work was supported by grants to R.M. from the National Science Foundation (Grant PCM 7907524) and the National Institutes of Health (Grant GM 29864). This paper is NRCC No. 20901.

[1] Abbreviations: DPPC, 1,2-dipalmitoyl-3-*sn*-phosphatidylcholine; DMPC-d_{54}, chain-perdeuterated 1,2-dimyristoyl-3-*sn*-phosphatidylcholine; Tris, tris(hydroxymethyl)aminomethane; DEGS, diethylene glycol succinate; DSC, differential scanning calorimetry; NANA, *N*-acetylneuraminic acid; FT-IR, Fourier transform infrared; DPPE, 1,2-dipalmitoyl-3-*sn*-phosphatidylethanolamine; T_m, temperature of the gel to liquid-crystal phase transition.

0006-2960/83/0422-1170$01.50/0

and dynamics of the lipid acyl chains so that the technique may be used to monitor lipid phase behavior directly without the possibility of structural perturbations induced by probe molecules. If one phospholipid component has its acyl chains perdeuterated, then the C–D stretching modes of the deuterated chains, which occur in a spectral region free from interference from other membrane components, may be monitored separately from the C–H modes of nondeuterated chains (Mendelsohn & Koch, 1980). Consequently, the conformation of each lipid component may be monitored in a single experiment.

The current study reports a FT-IR investigation of the reconstitution of glycophorin into lipid mixtures of DPPC–DMPC-d_{54}. The protein is a well-characterized transmembrane protein that can be isolated in reasonable quantities (Marchesi & Andrews, 1971) and reconstituted in straightforward fashion into both the gel and liquid-crystalline lipid phases (MacDonald & MacDonald, 1975), although exhibiting a preference for the latter (MacDonald, 1980). The particular lipid mixture (with nondeuterated acyl chains) has been studied with a variety of physical methods (Shimshick & McConnell, 1973; Chapman et al., 1974; Lee, 1975); phase behavior deduced from the current FT-IR data may then be directly compared with the earlier work. Previous Raman and FT-IR studies (Taraschi & Mendelsohn, 1980; Mendelsohn et al., 1981) of lipid–protein interaction in the glycophorin–DMPC system demonstrated that an increase in the protein concentration results in a gradual increase in lipid disorder with no evidence for immobilized boundary lipid; therefore the current data are treated according to a simple two-state model. This allows the determination of the fraction of each lipid component melted both in the binary mixture alone and in the presence of protein as well as the construction of approximate phase diagrams.

Materials and Methods

Materials. DPPC was purchased from Sigma Chemical Co. (St. Louis, MO) and checked for purity by TLC. DMPC-d_{54} was purchased from Serdary Research Laboratories (London, Ontario, Canada) and purified on a Sephadex LH-20 column.

Neuraminidase from *Clostridium perfringens* (type VI) and trypsin were purchased from Sigma. Sepharose 4B and Sephadex LH-20 were products of Pharmacia Fine Chemicals (Piscataway, NJ).

Sample Preparation. Glycophorin was prepared from human erythrocytes by using methods previously described in detail (Mendelsohn et al., 1981). Briefly, hemoglobin-free erythrocyte ghosts prepared by hypotonic lysis (Dodge et al., 1963) were disrupted with lithium diiodosalicylate (Marchesi & Andrews, 1971) and the proteins extracted with phenol. The crude protein preparation was treated with $CHCl_3$–MeOH and EtOH to remove remaining bound lipid. Polyacrylamide gel electrophoresis of the resulting protein gave patterns consistent with those previously published (Furthmayer et al., 1975).

Glycophorin was incorporated into binary lipid vesicles according to the procedure of MacDonald & MacDonald (1975). Measured amounts of protein and the two lipid species were simultaneously solubilized in $CHCl_3$–MeOH–H_2O (6.5:2.5:0.4 v/v/v) and solvent removed by N_2 drying followed by overnight evacuation. The lipid–protein film was rehydrated in 1.26 M NaCl–0.01 M Tris, pH 7.5, and vesicles were collected by centrifugation at 2×10^4 rpm for 1 h. Lipid phosphorus was determined by the method of Chen et al. (1956), while glycophorin was determined as sialic acid by the method of Warren (1959). Reconstitution of lipid–protein complexes in D_2O was accomplished as described above except that the rehydration buffer was 1.26 M NaCl–0.01 M Tris in D_2O, pD 7.5.

Sample Characterization. Vesicles were assayed for lipid chain length distribution by gas chromatography of their methylated acyl chains. The vesicle lipids were transesterified with 5% (w/w) HCl in MeOH and extracted with petroleum ether (bp 30–60 °C). The methyl esters were then analyzed on a Hewlett-Packard 5750 gas chromatograph equipped with a column of 5% DEGS on Chromosorb W, 80–100 mesh, by using a temperature program of 80–210 °C.

Association of lipid and protein in the vesicles was assayed by column chromatography on Sepharose 4B. Aliquots of 0.20 mL were applied to a column (0.9 × 20.0 cm) equilibrated in 0.13 M NaCl–0.01 M Tris, pH 7.5, and fractions were eluted at room temperature. Lipid concentration in the fractions was determined from phosphorus determination (Chen et al., 1956) and protein concentration from sialic acid determination (Warren, 1959).

Asymmetry of protein incorporation in the vesicles was assayed either by (i) exposure to neuraminidase (0.10 unit at 1 unit/mL) or by (ii) trypsin cleavage (5% w/w) of the exposed polypeptide. In both cases the vesicles were centrifuged and the resultant solution was analyzed for sialic acid.

Negative-stain electron microscopy was performed on a Phillips EM 200 operating at 80 kV with an initial magnification of 12000–44000×. Vesicles in 0.05 M Tris, pH 7.5, were placed on a Formvar-filmed and heavily carbon coated grid for 5 min and the excess was blotted off. Phosphotungstic acid (1%) was added for 5 min and the preparation air-dried before use.

Fourier Transform Infrared Spectroscopy. Samples were prepared for infrared spectroscopy in 50 μm thick cells with CaF_2 windows. Spectra were recorded on a Digilab FTS-11 Fourier transform infrared spectrometer equipped with a HgCdTe detector. Six hundred interferograms, collected with an optical velocity of 1.26 cm s^{-1} and a maximum optical retardation of 0.25 cm, were coadded, apodized with a triangular function, and Fourier transformed with one level of zero filling to yield a resolution of 4 cm^{-1} and data encoded every 2 cm^{-1}.

Temperatures were controlled by a thermostated EtOH–H_2O mixture flowing through a hollow cell mount and monitored by a copper–constantan thermocouple placed against the edge of the cell window (Cameron & Jones, 1981).

Frequencies were determined with an uncertainty of less than ±0.1 cm^{-1} by computing centers of gravity of bands by using the topmost three data points (Cameron et al., 1982b).

For determination of the widths of C–D stretching bands, samples in H_2O were studied. The "water-association" band at ~2150 cm^{-1} was subtracted and bandwidths were determined relative to a straight base line extending from 2125 to 2025 cm^{-1}. For determination of the widths of C–H stretching bands, samples in D_2O were studied. The sloping base line caused by the high-frequency side of the strong O–D stretching band was subtracted and the bandwidths were determined relative to a straight base line extending from 2880 to 2820 cm^{-1}. The subtraction of the background caused by H_2O or D_2O bands was performed by using spectra of H_2O or D_2O recorded at the same temperature as those of the samples under study (Cameron et al., 1979). Uncertainties in bandwidth values are less than ±0.2 cm^{-1}.

Results

Biochemical Characterization of Complexes. Lipid–protein complexes formed according to the procedure of MacDonald

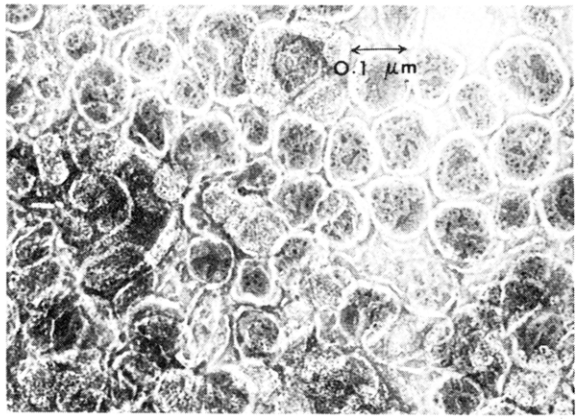

FIGURE 1: Typical electron micrographs of DPPC–DMPC-d_{54}–glycophorin vesicles. Magnification is 39375×. The size distribution (1000–1200-Å diameter) is typical of all preparations used in the current work.

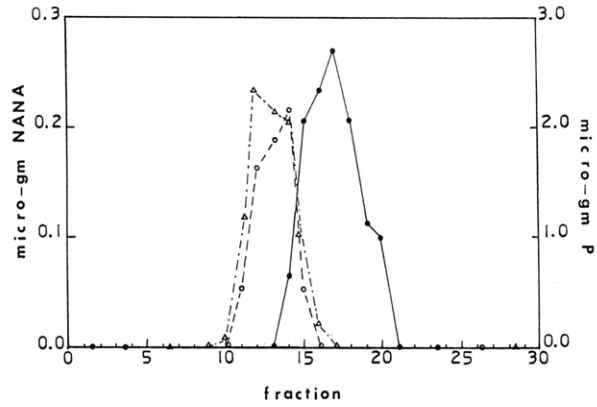

FIGURE 2: Elution profile from a Sepharose 4B column of free glycophorin (●) as compared with vesicle-bound glycophorin (○) and lipid (△). Free glycophorin was dissolved in 0.13 M NaCl–0.01 M Tris-HCl, pH 7.5, at a concentration of 6.25 mg mL^{-1} and passed through the column. Fractions were assayed for sialic acid. Vesicles prepared as described under Materials and Methods were suspended in 0.13 M NaCl–0.01 M Tris-HCl, pH 7.5, at a concentration of 11.67 mg mL^{-1} for lipid and 5.99 mg mL^{-1} for protein and passed over the column; fractions were analyzed both for sialic acid and phosphorus. Fractions were eluted at room temperature at a rate of 12 mL h^{-1}.

and MacDonald (1975) lead to a relatively homogeneous population of large unilamellar vesicles (Figure 1) with a size distribution as measured from the electron micrographs of 0.1–0.12 μm. Evidence for complex formation is obtained from gel exclusion chromatography on Sepharose 4B (Figure 2). When the lipid–protein preparation is chromatographed, the glycophorin coelutes with phospholipid and has a significantly shorter retention time than uncomplexed protein. In addition, the electron microscopy studies show that no multilamellar vesicles are formed during the complexation. Cleavage of those portions of the protein external to the vesicle with trypsin or neuraminidase followed by sialic acid determination suggests that 90% of the sialic acid residues are oriented toward the exterior. This level of asymmetry is slightly higher than that reported by van Zoelen et al. (1978a,b) but consistent with that of Ong et al. (1981).

The lipid compositions and lipid–protein ratios of the complexes examined in the FT-IR experiments are given in Table I. Samples A (A′), B (B′), and C (C′) refer to low, medium, and high mole fractions of DPPC in the H_2O (D_2O) suspension. Two points bear comment. Attempts to prepare complexes at high DMPC-d_{54} levels (mole fractions of 0.8) led to complexes with less DMPC-d_{54} present. In addition, the incorporation of glycophorin into the vesicles was slightly enhanced when D_2O rather than H_2O was used in the rehydration buffer. Lipid standards for the spectroscopic studies were made up at the same mole ratios as those in the ternary systems.

Table I: Composition of DPPC–DMPC-d_{54}–Glycophorin Complexes for FT-IR Studies[a]

sample[b]	DPPC:DMPC-d_{54} mole ratio	lipid:protein mole ratio	solvent
A	29:71	96:1	H_2O
A′	34:66	80:1	D_2O
B	55:45	114:1	H_2O
B′	52:48	85:1	D_2O
C	79:21	96:1	H_2O
C′	77:23	76:1	D_2O

[a] Estimated errors: 3% in lipid:lipid and 5% in lipid:protein mole ratios. [b] Samples of binary lipid mixtures without protein were made up at the same mole ratios as for the protein-containing complexes. These are referred to as lipid standards.

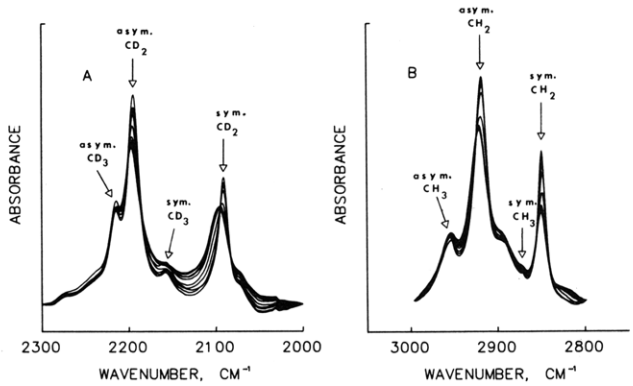

FIGURE 3: Temperature dependence of the infrared spectra of (A) the C–D stretching region (lipid standard B from Table I) and (B) the C–H stretching region of a DPPC–DMPC-d_{54} binary mixture (lipid standard B′ from Table I). Spectra decrease in peak height with increasing temperature and are plotted in intervals of ~5 °C over the range 10–60 °C. In the case of (A) the broad "water-association" band at ~2150 cm^{-1} has been subtracted; in the case of (B) the high-frequency side of the O–D stretching band has been subtracted. For the purpose of display, linear base lines extending from 2300 to 2000 cm^{-1} in (A) and from 3000 to 2800 cm^{-1} in (B) have been used.

Infrared Spectroscopy. The temperature dependence of the C–D and C–H stretching regions for lipid standards B and B′ (Table I) are shown in parts A and B of Figure 3, respectively. The CD_3 groups of DMPC-d_{54} give rise to bands (Figure 3A) at 2212 (asymmetric stretch) and at 2169 and 2070 cm^{-1} (symmetric stretch) while the stronger bands at 2194 and 2089 cm^{-1} are the antisymmetric and symmetric CD_2 stretching modes respectively (Cameron et al., 1981). The five spectral features in Figure 3B arise from the nondeuterated acyl chains of DPPC. The asymmetric and symmetric CH_3 stretching modes appear near 2956 and 2872 cm^{-1} (Cameron et al., 1980) while the antisymmetric and symmetric CH_2 stretching bands are observed at 2920 and 2850 cm^{-1} along with a broad Fermi resonance band (Snyder et al., 1978) centered at about 2900 cm^{-1}.

Variations in temperature produce changes in line width and frequency position in both spectral regions which occur over a temperature interval significantly wider than that for the pure lipid components. This is the type of melting behavior expected for a binary lipid system with miscibility in both solid and liquid phases (Lee, 1977). The temperature-induced variation in the symmetric CH_2 stretching frequency for various lipid binary mixtures is shown in Figure 4. Plots of the half-width (full width at half-height) for the same vibra-

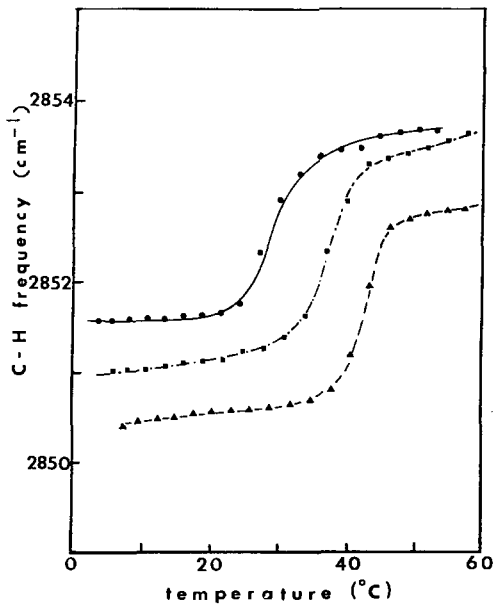

FIGURE 4: Plots of frequency vs. temperature for the symmetric CH_2 stretching band at 2850 cm^{-1} in DPPC–DMPC-d_{54} multilayers as a function of mole fraction of DPPC [(●) = 0.34, (■) = 0.52, and (▲) = 0.77 mole fraction of DPPC].

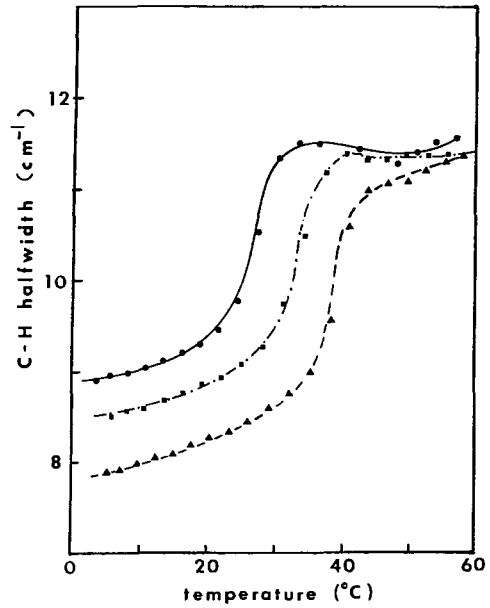

FIGURE 5: Plots of the full width at half maximum intensity vs. temperature for the symmetric CH_2 stretching band at 2850 cm^{-1} in DPPC–DMPC-d_{54} multilayers as a function of mole fraction of DPPC [(●) = 0.34, (■) = 0.52, and (▲) = 0.77 mole fraction of DPPC].

tional mode are shown in Figure 5. Similar data (not shown) were obtained for the symmetric CD_2 stretching frequency and bandwidth as a function of temperature for all the lipid–protein complexes and for all the lipid standards listed in Table I.

Spectral Analysis. The FT-IR spectroscopic parameters normally used to characterize lipid phase transitions are the frequency and width of acyl chain C–H and C–D stretching bands (Cameron et al., 1980). Figure 6 shows the temperature dependence of the frequency and half-width of the symmetric CD_2 stretching mode for sample C as an example of their behavior. It is immediately apparent from Figure 6 that the changes in frequency and width are not concerted and that the maximum rate of change of the width occurs at a lower temperature than that of the frequency. Furthermore, the

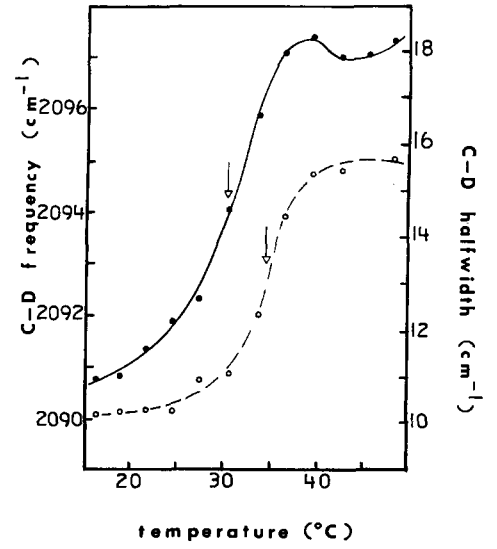

FIGURE 6: Plot of the temperature dependence of the frequency (○) and half-width (●) of the symmetric CD_2 stretching mode at 2089 cm^{-1} for sample C 79:21 (h_{62}:d_{54})–glycophorin (96:1) in H_2O. Arrows indicate points of maximal inflection in the melting curves.

melting curve constructed with the half-width data shows a maximum before the completion of the melting. This distinct behavior for frequency and bandwidth has been observed previously in melting curves for bacterial membranes (Casal et al., 1980, 1982) and in the coagel to micelle transition of several surfactants (Sapper et al., 1981; Cameron et al., 1982a).

Previous explanations of the temperature dependencies of the bandwidth and frequency parameters assumed that each responds to different aspects of lipid order and mobility (Cameron et al., 1980; Casal et al., 1980, 1982). While this assumption may be correct, it is now apparent that these two parameters do not change in a concerted fashion when the transformation involves the coexistence of two phases with different bandwidths. Umemura et al. (1980, 1981) have studied the characteristics of band contours resulting from the overlap of two Lorentzian lines with different bandwidths. They have shown that the temperature-induced variation in bandwidth and frequency are not concerted and that plots similar to those in Figure 6 can be obtained by the superposition of two Lorentzian bands whose frequency separation is much smaller than their half-widths.

To analyze the present data quantitatively, a two-state model was assumed for each of the lipid components similar to the approach used to analyze the infrared spectral changes observed at the monomer–micelle transition of aqueous sodium *n*-alkanoates (Umemura et al., 1981). Changes in the measured bandwidths or frequencies are not linear functions of the fraction of lipid transformed; in addition, the functional form for the variation in frequency with the fraction transformed is different from that for the variation in bandwidth. If A_G = the concentration of gel-state A and A_L = the concentration of liquid-crystalline A with similar expressions for lipid component B, then the model assumes that at all temperatures, a maximum of two classes of each lipid exists:

$$A_G \rightleftarrows A_L$$

$$B_G \rightleftarrows G_L$$

It is further assumed that the shapes of the C–H or C–D stretching bands characterizing the pure gel or pure liquid-crystalline states are adequately represented by a Lorentzian distribution (Ramsay, 1952), with characteristic frequency and half-width extrapolated from the low temperature linear region

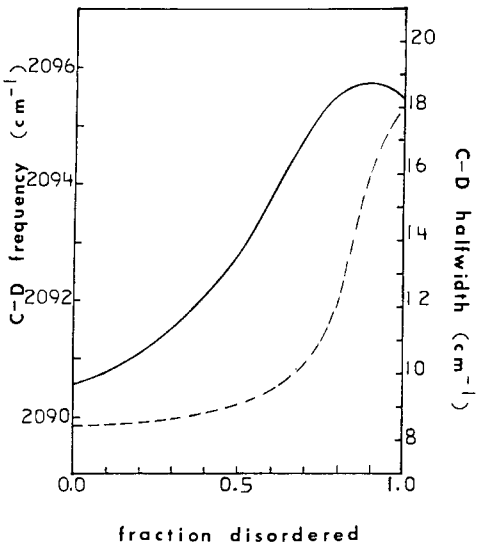

FIGURE 7: Calculated variation in frequency (---) and half-width (—) as a function of the extent of melted lipid for the DMPC-d_{54} component of sample C (composition as in Figure 6). Lorentzian band shapes for the totally solid (0.0 fraction disordered) and totally liquid (1.0 fraction disordered) components are generated. Addition of the two band shapes in varying proportions leads to intermediate band shapes of characteristic frequency and half-width, as shown.

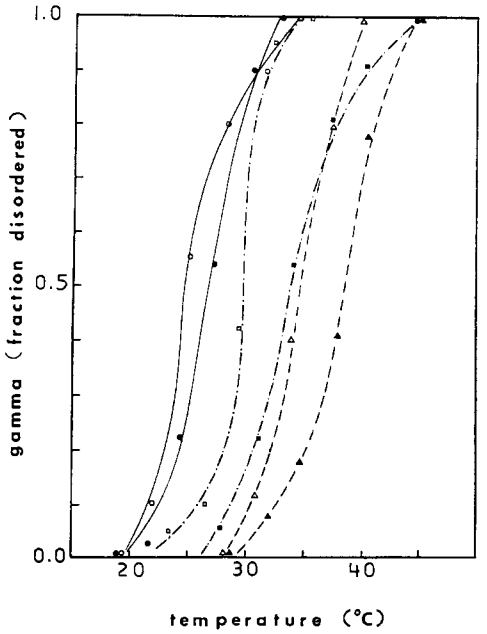

FIGURE 8: Plots of γ (i.e., fraction of disordered lipid) vs. temperature for the DPPC component. Standard A′, 34% DPPC (●); sample A′, 34% DPPC with protein (○); standard B′, 52% DPPC (■); sample B′, 52% DPPC with protein (□); standard C′, 77% DPPC (▲); sample C′, 77% DPPC with protein (△).

of the melting curve (for the gel phase) or the high-temperature linear region (for the liquid-crystalline phase). The observed spectrum for a given component at temperatures intermediate between these regions is the superposition of the gel-phase spectrum and the liquid-crystalline spectrum, the relative proportion of the latter increasing with temperature. The details are outlined in the Appendix.

Typical variations in frequency and half-width as a function of fractional lipid melting as calculated with this model are given in Figure 7 for sample C (lipid:protein mole ratio 96:1; lipid composition DPPC–DMPC-d_{54}, 79:21). The results confirm that neither parameter varies linearly as the broadened gel–liquid-crystalline phase transition proceeds. Changes in the frequency are typically very slight until 70–80% of the lipid has melted at which point a more drastic variation is noted. In contrast, the half-width changes much more significantly in the range 0–75% lipid melted and at high values goes through a maximum. Nevertheless, the half-width is the preferred parameter for data analysis as a slight error in the frequency measurement could lead to a large error in the fraction of a particular lipid component melted. The apparent difference observed in melting behavior according to whether the frequency or half-width is plotted vs. temperature may be traced to the widely different responses these parameters have to lipid melting (Figure 7).

Phase Diagram Construction. Elucidation of phase behavior in lipid mixtures requires the construction of phase diagrams (Lee, 1977) based on either the set of onset and completion temperatures experimentally determined as a function of composition or a theoretical expression derived from a variant of solution theory using the molar enthalpies of the pure components along with (possibly) several parameters defining the departure of the system from ideality. Neither approach is appropriate for the current work. As is clear from Figure 6, the selection of reasonable onset and completion temperatures is somewhat arbitrary. In addition, since the two lipid components melt to different extents at a particular temperature once melting has commenced, it is inappropriate to assign an onset or completion temperature for the system as a whole from data for a single component. The second method of phase diagram construction suffers from an a priori lack of knowledge of the nonideality parameters. On the basis of the computer simulation results, it was decided to construct phase diagrams from those FT-IR data that clearly lie within the two-phase region for each lipid component. The method is outlined in the Appendix.

The method requires determination of the fraction of each fraction of each lipid component melted (see eq 1 in the Appendix). This is accomplished with a procedure essentially inverted from that used to generate Figure 7. A particular value for the fraction of each lipid component melted is chosen so that the experimentally determined half-width at a given temperature is reproduced.

The fraction of lipid melted, γ_1 or γ_2, can be used to monitor the response of each component to the introduction of protein. Figures 8 and 9 show γ for the DPPC and DMPC-d_{54} components, respectively, both alone and in the presence of glycophorin.

The values for γ are inserted into eq 2 to yield phase diagrams for the binary lipid mixture (Figure 10) and the ternary system (Figure 11). Incorporation of glycophorin results in a phase diagram in which the liquids line is significantly lowered compared with that of the binary system. The solidus line is essentially unchanged.

Discussion

The current study allows two questions to be addressed: (a) What is the effect of glycophorin on the phase behavior of the DMPC-d_{54}–DPPC mixture? (b) Does glycophorin preferentially partition into a region of particular chain length in the above lipid mixture? The phase diagram for the binary mixture (Figure 10) is similar to those in the literature constructed from a variety of techniques for the DMPC–DPPC system (Shimshick & McConnell, 1973; Chapman et al., 1974; Lee, 1975). Acyl chain perdeuteration of the DMPC component results in a ~5 °C lowering of T_m for the pure component but leads to little change in the shape in the phase diagram of the mixture. These results show that chain perdeuteration does not severely perturb lipid phase behavior,

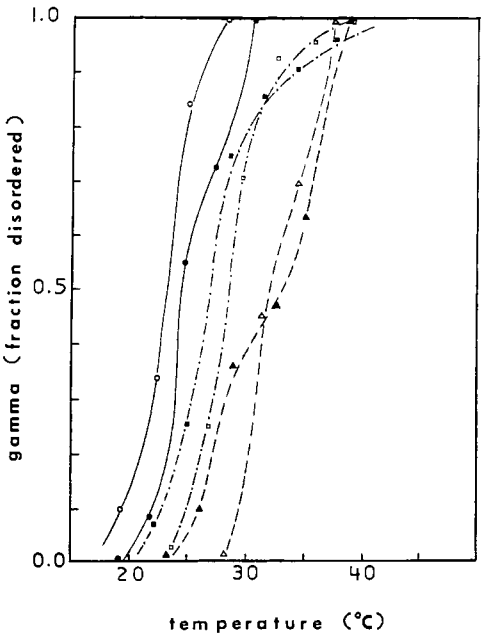

FIGURE 9: Plots of γ (i.e., fraction of disordered lipid) vs. temperature for the DMPC-d_{54} component. Standard A, 71% DMPC-d_{54} (●); sample A, 71% DMPC-d_{54} with protein (○); standard B, 45% DMPC-d_{54} (■); sample B, 45% DMPC-d_{54} with protein (□); standard C, 21% DMPC-d_{54} (▲); sample C, 21% DMPC-d_{54} with protein (△).

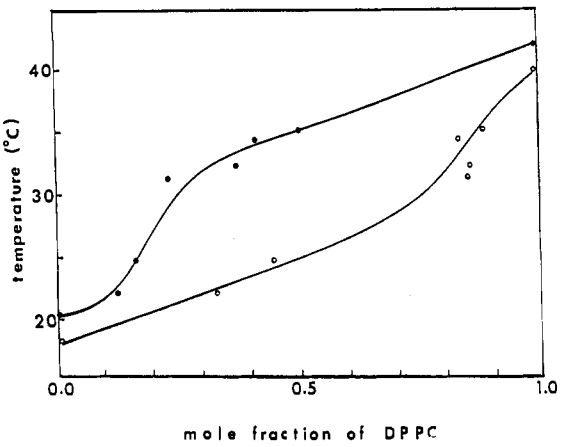

FIGURE 10: Phase diagram calculated for the binary lipid mixture DPPC–DMPC-d_{54} by using methods outlined in the Appendix. The melting temperatures at the end points (0.0 and 1.0 mol fraction of DPPC) were determined from FT-IR melting curves of the pure lipids DMPC-d_{54} and DPPC, respectively.

consistent with earlier studies. Gaber et al. (1978) and Klump et al. (1981) showed that chain perdeurated DPPC behaves as a normal phosphatidycholine molecule, having both a pretransition and a main chain melt; mixtures of DPPC and DPPC-d_{62} showed ideal behavior. In addition, Mendelsohn & Koch (1980) showed that the nonideality parameters used to describe the mixing behavior of DPPC-d_{62} and DPPE were similar to those for DPPC and DPPE, so that chain perdeuteration did not greatly affect the enthalpy of interchain interaction.

DMPC-d_{54} and DPPC show complete miscibility in both gel and liquid-crystalline phases, although the shape of the phase diagram differs from that expected for an ideal mixture. Incorporation of glycophorin at the level of about 1 mol % causes a lowering of the liquidus line while leaving the solidus line virtually unchanged (Figure 10 and 11). Such behavior is consistent with the reduction of the enthalpy of melting of the components (Reisman, 1970), which in the current case

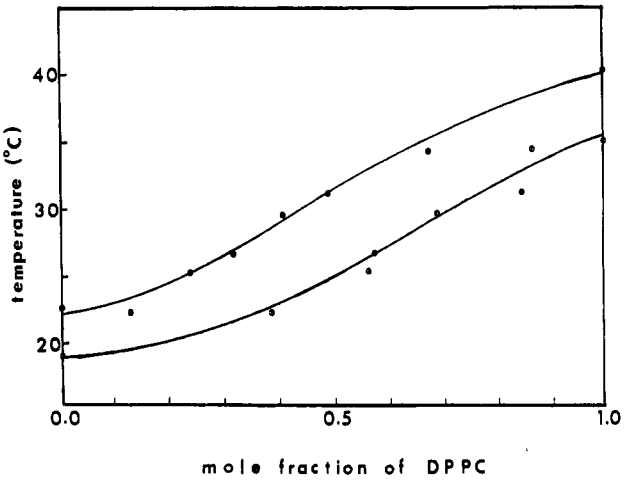

FIGURE 11: Phase diagram calculated for the ternary system DPPC–DMPC-d_{54}–glycophorin by using methods outlined in the Appendix. The melting temperatures at the end points (i) 0.0 mole fraction of DPPC (corresponding to DMPC-d_{54}), and (ii) 1.0 mole fraction DPPC of were determined from FT-IR melting curves of a 100:1 DMPC-d_{54}–glycophorin complex and a 100:1 DPPC–glycophorin complex, respectively (R. Dluhy, R. Mendelsohn and H. Casal, unpublished observations).

is best referred to glycophorin complexed with a single lipid at the level of about 1 mol %. The reduction in enthalpy of transition during the interaction of hydrophobic proteins with a single lipid component has been experimentally demonstrated with differential scanning calorimetry (Boggs et al., 1977a,b; van Zoelen et al., 1978a,b).

The phase diagram for the ternary system (Figure 11) also shows that glycophorin does not induce phase separation in the lipid mixture, as indicated by the absence of monotectic behavior in the presence of protein. In previous studies (Boggs et al., 1977a,b), specific interactions between charged lipids and proteins were responsible for protein-induced lipid phase separations. Such events, mediated by different lipid head groups, cannot occur in the present case.

The model of lipid phase behavior assumed here permits determination of the extent to which each lipid component melts (Figures 8 and 9). The primary result of glycophorin incorporation is enhancement of melting of the DPPC in the ternary system compared with the binary phospholipid mixture, the effect being observed at all lipid compositions. For DMPC-d_{54}, this effect is noted only at high mole fractions. It appears that glycophorin tends to disorder and/or fluidize gel-phase phosphatidylcholines, the magnitude of the interaction depending upon the chain length. These conclusions are consistent with observations from Raman spectroscopy (R. Mendelsohn and R. Dluhy, unpublished experiments) that acyl chain packing in the gel phase is disrupted by glycophorin. Lipid miscibility in well-mixed systems is not expected to be greatly affected by this fluidization process. It might be expected, however, that binary lipid mixtures which behave monotectically would mix in the presence of glycophorin.

The two-state model adopted in the current work is the simplest consistent with the data. The approach does not invoke the existence of a layer of motionally restricted ("boundary") lipid in the immediate vicinity of protein, an assumption consistent with earlier FT-IR and Raman investigations (Taraschi & Mendelsohn, 1980; Mendelsohn et al., 1981). More elaborate versions of the current model (involving perhaps a distribution of lipid states) will have to await the systematic study of a variety of more complicated ternary and binary systems whose phase behavior as determined calorimetrically may be compared with that developed from the

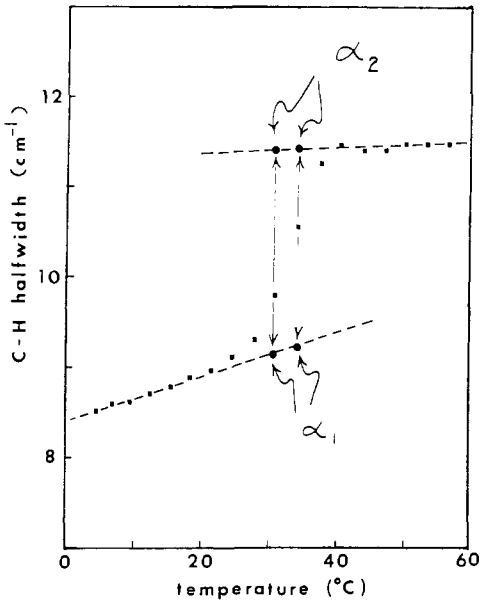

FIGURE 12: Generation of the half-width parameter used in the Lorentzian band shape simulations. The example illustrated is that of the DPPC component of lipid standard B [DPPC–DMPC-d_{54} (55:45)]. The low- and high-temperature melting data are extrapolated forward and backward, respectively, through the melting region. The halfwidth parameters used in the simulation of the Lorentzian band shape corresponding to the gel phase (α_1) and the liquid-crystalline phase (α_2) at particular temperatures through the melting region are taken from the extrapolated lines. This procedure is repeated for all the half-width and frequency parameters for both DPPC and DMPC-d_{54} for all samples and standards.

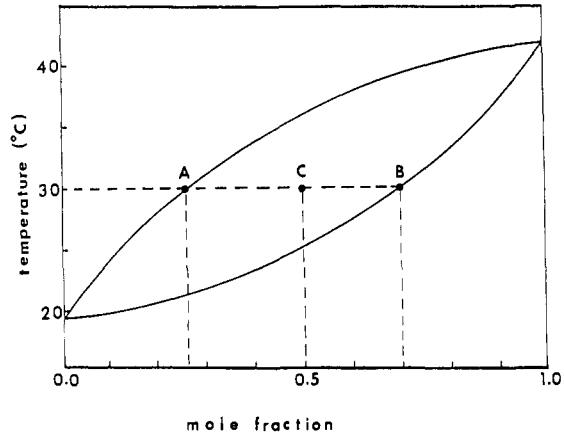

FIGURE 13: Typical ascending phase diagram for a binary mixture displaying miscibility in both the solid and liquid states. At any temperature within the two-phase region, a tie line (e.g., A–B) can be drawn and the following points defined: A = composition of the liquid phase at a temperature T; B = composition of the solid phase at T; C = mole fraction of component 1 in the system.

current protocol. If necessary, these more elaborate schemes could include a layer or two of lipid molecules in the immediate vicinity of protein, with spectral characteristics altered from those of the bulk lipids. Such a procedure has been used by Lentz et al. (1982) to account for diphenylhexatriene fluorescence anisotropy data in native sarcoplasmic reticulum vesicles.

The validity of the current approach rests on the fact that different lipid physical states have measurably different spectral characteristics. For the simple phase diagrams studied here, the FT-IR spectral alterations of a particular lipid class between gel and liquid-crystalline phases are quite marked. However, for phase diagrams of a more complex nature, involving perhaps lateral separations and compound formation, there may be only slight changes in lipid order and/or fluidity from one phase to the next. The FT-IR approach in such a circumstance might not sense all of the phases that occur. This problem is currently being investigated with lipid mixtures known to have complex phase characteristics.

Acknowledgments

We thank D. G. Cameron for stimulating discussions.

Appendix

A Description of the Model Used To Generate Phase Diagrams from FT-IR Data. (A) Spectral Simulations. Computer simulation of the FT-IR spectra for a lipid C–H or C–D stretching band was based on the assumption that at temperatures within the two phase region, the observed spectrum was a superposition of two Lorentzians, corresponding to gel and liquid-crystalline lipid. A procedure analogous to that of Heyn et al. (1981) used to treat fluorescence data was adapted for the current study. Lorentzian parameters (bandwidths and frequencies) for hypothetical pure gel and liquid-crystalline states of lipid at particular temperatures within the two-phase region were generated by extrapolation from the linear low- and high-temperature regions of the melting curves as shown in Figure 12. The experimentally measured half-width for a particular lipid component band was then reproduced by simulating an experimental spectrum according to eq 1 by using the derived Lorentzian parameters:

$$I(\nu) = (1-\gamma)\left[\frac{1}{1+2(\nu-\nu_1)^2/\alpha_1}\right] + \beta\gamma\left[\frac{1}{1+2(\nu-\nu_2)^2/\alpha_2}\right] \quad (1)$$

$I(\nu)$ = intensity as a function of frequency, γ = fraction of disordered lipid, ν_1 = peak frequency for the gel-state lipid, α_1 = half-width for the gel-state Lorentzian, β = peak height of the liquid-crystalline-state band relative to that of the gel-state band, ν_2 = peak frequency for the liquid-crystalline lipid, and α_2 = half-width for the liquid-crystalline-state Lorentzian.

γ is varied until the half-width of the calculated spectrum matches the experimental halfwidth. We note that β, the ratio of peak height of liquid-crystalline- to gel-state bands, is not an indicator of concentration. It is only a scaling parameter determined experimentally and used to ensure that the gel and liquid-crystalline bands are added in the proper proportion. The difference between this procedure and that of Heyn et al. (1981) is that the necessity for assuming a linear relationship between the experimental parameter (half-width in this case) and the fraction of lipid melted is avoided.

(B) Phase Diagram Construction. A typical phase diagram for a system displaying complete miscibility in the gel and liquid-crystalline states is shown in Figure 13. The following points are defined on the composition axis for the indicated tie line: $A = (N_{1L})(N_{1L} + N_{2L})^{-1}$, the composition of the liquid phase at temperature T; $B = (N_{1S})(N_{1S} + N_{2S})^{-1}$, the composition of the solid phase at temperature T; $C = (N_{1L} + N_{1S})(N_{1L} + N_{1S} + N_{2S} + N_{2L})^{-1}$, the mole fraction of component 1 in the system. N_{1S} = moles of component 1 in the gel phase, N_{2S} = moles of component 2 in the gel phase, N_{1L} = moles of component 1 in the liquid-crystalline state, and N_{2L} = moles of component 2 in the liquid-crystalline state. The results of the spectral simulations yield quantities representing the fraction of each lipid component melted γ_1 and γ_2, i.e., $\gamma_1 = N_{1L}(N_{1L} + N_{1S})^{-1}$, the fraction of the liquid-crystalline phase of component 1 at temperature T, and $\gamma_2 = N_{2L}(N_{2L} + N_{2S})^{-1}$, the fraction of the liquid-crystalline phase of com-

ponent 2 at temperature T. It is easily shown that equations for liquidus (A) and solidus (B) temperature-specific compositions in terms of the observable quantities γ_1, γ_2, and C are

$$A = \gamma_1 C[C(\gamma_1 - \gamma_2) + \gamma_2]^{-1}$$
$$B = C(1 - \gamma_1)[C(\gamma_2 - \gamma_1) + (1 - \gamma_2)]^{-1} \quad (2)$$

The use of the quantities γ in eq 1 for each component results in a set of points defining the liquidus and solidus curves of the phase diagrams as constructed in Figures 10 and 11.

Registry No. DPPC, 63-89-8; DMPC, 18194-24-6.

References

Boggs, J. M., Wood, D. D., Moscarello, M. A., & Papahadjopoulos, D. (1977a) *Biochemistry 16*, 2325–2329.

Boggs, J. M., Moscarello, M. A., & Papahajopoulos, D. (1977b) *Biochemistry 16*, 5420–5426.

Cameron, D. G., & Jones, R. N. (1981) *Appl. Spectrosc. 35*, 448–452.

Cameron, D. G., Casal, H. L., & Mantsch, H. H. (1979) *J. Biochem. Biophys. Methods 1*, 21–36.

Cameron, D. G., Casal, H. L., & Mantsch, H. H. (1980) *Biochemistry 19*, 3665–3672.

Cameron, D. G., Casal, H. L., Mantsch, H. H., Boulanger, Y., & Smith, I. C. P. (1981) *Biophys. J. 35*, 1–16.

Cameron, D. G., Umemura, J., Wong, P. T. T., & Mantsch, H. H. (1982a) *Colloids Surf. 4*, 131–145.

Cameron, D. G., Kauppinen, J. K., Moffatt, D. J., & Mantsch, H. H. (1982b) *Appl. Spectrosc. 36*, 245–250.

Casal, H. L., Cameron, D. G., Smith, I. C. P., & Mantsch, H. H. (1980) *Biochemistry 19*, 444–451.

Casal, H. L., Cameron, D. G., Jarrell, H. C., Smith, I. C. P., & Mantsch, H. H. (1982) *Chem. Phys. Lipids, 30*, 17–26.

Chapman, D., Urbina, J., & Keough, K. M. (1974) *J. Biol. Chem. 249*, 2512–2521.

Chapman, D., Cornell, B. A., Eliasz, A. W., & Perry, A. (1977) *J. Mol. Biol. 113*, 517–538.

Chen, P. S., Toribara, T. Y., & Warner, H. (1956) *Anal. Chem. 28*, 1756–1758.

Dodge, J. T., Mitchell, C., & Hanahan, D. J. (1963) *Arch. Biochem. Biophys. 100*, 119–130.

Furthmayer, H., Tomita, M., & Marchesi, V. T. (1975) *Biochem. Biophys. Res. Commun. 65*, 113–121.

Gaber, B. P., Yager, P., & Peticolas, W. (1978) *Biophys. J. 22*, 191–207.

Heyn, M. P., Blume, A., Rehorek, M., & Dencher, N. A. (1981) *Biochemistry 20*, 7109–7115.

Jonas, A., & Mason, W. R. (1981) *Biochemistry 20*, 3801–3805.

Kleeman, W., Grant, C. W. M., & McConnell, H. M. (1974) *J. Supramol. Struct. 2*, 609–616.

Klump, H. H., Gaber, B. P., Peticolas, W. L., & Yager, P. (1981) *Thermochim. Acta 48*, 361–366.

Lee, A. G. (1975) *Biochim. Biophys. Acta 413*, 11–23.

Lee, A. G. (1977) *Biochim. Biophys. Acta 472*, 285–344.

Lentz, B. R., Moore, B. M., Kirkman, C., & Meissner, G. (1982) *Biophys. J. 37*, 30–32.

MacDonald, R. I. (1980) *Biochim. Biophys. Acta 597*, 189–192.

MacDonald, R. I., & MacDonald, R. C. (1975) *J. Biol. Chem. 250*, 9206–9214.

Marchesi, V. T., & Andrews, E. P. (1971) *Science (Washington, D.C.) 174*, 1247–1248.

Mendelsohn, R., & Koch, C. (1980) *Biochim. Biophys. Acta 598*, 260–271.

Mendelsohn, R., Dluhy, R., Taraschi, T., Cameron, D., & Mantsch, H. H. (1981) *Biochemistry 20*, 6699–6706.

Ong, R. L., Marchesi, V. T., & Prestegard, J. Y. (1981) *Biochemistry 20*, 4283–4292.

Parsegian, A., Ed. (1982) *Biophysical Discussions; Protein-Lipid Interactions in Membranes*, Rockefeller University Press, New York.

Ramsay, D. A. (1952) *J. Am. Chem. Soc. 74*, 72–80.

Reisman, A. (1970) *Phase Equilibria*, Academic Press, New York.

Sapper, H., Cameron, D. G., & Mantsch, H. H. (1981) *Can. J. Chem. 59*, 2543–2549.

Shimshick, E. J., & McConnell, H. M. (1973) *Biochemistry 12*, 2351–2360.

Snyder, R. G., Hsu, S. L., & Krimm, S. (1978) *Spectrochim. Acta, Part A 34A*, 395–406.

Taraschi, T., & Mendelsohn, R. (1980) *Proc. Natl. Acad. Sci. U.S.A. 77*, 2362–2366.

Umemura, J., Cameron, D. G., & Mantsch, H. H. (1980) *J. Phys. Chem. 84*, 2272–2277.

Umemura, J., Mantsch, H. H., & Cameron, D. G. (1981) *J. Colloid Interface Sci. 83*, 558–568.

van Zoelen, E. J. J., Van Dijck, P. W. M., De Kruiff, B., Verkleij, A. J., & Van Deenen, L. L. M. (1978a) *Biochim. Biophys. Acta 514*, 9–24.

van Zoelen, E. J. J., Verkleij, A. J., Zwaal, R. F. A., & Van Deenen, L. L. M. (1978b) *Eur. J. Biochem. 86*, 539–546.

Verma, S. P., Wallach, D. F. H., & Sakura, J. D. (1980) *Biochemistry 19*, 574–579.

Warren, L. (1959) *J. Biol. Chem. 234*, 1971–1975.